

# Temperature Sensorless Thermal Management Strategy for Interleaving Power Converters

Zehui Li, Mingde Zhou, and Haoyu Wang  
 School of Information Science and Technology  
 ShanghaiTech University, Shanghai, China

Shanghai Engineering Research Center of Energy Efficient and Custom AI IC  
 wanghy@shanghaitech.edu.cn

**Abstract**— Conventionally, to achieve thermal balance in interleaving power conversion systems, temperature sensor-based closed-loop control is required. However, temperature sensing is typically slow and cannot accurately measure the junction temperature of power semiconductors in real-time. To resolve this issue, this paper proposes a novel thermal management strategy for interleaving power converters. It is based on the weighted current sharing strategy and gets rid of the temperature sensors. The loss model of power semiconductors is established to characterize the thermal performance. Fast closed-loop control is implemented to achieve thermal balance. To verify the proposed concept, a two-phase interleaved buck converter is designed to serve as the case study. The results show that 1) the designed prototype can regulate the output voltage tightly to the reference; 2) the output currents of each module are balanced utilizing a current-sharing loop; 3) thermal balance without temperature-sensing is achieved using the proposed loss-sharing-loop.

**Keywords**— Active thermal control, current sharing, interleaving power converters.

## I. INTRODUCTION

With the rapid development of microprocessor technology, modern processors are facing the challenge of "low voltage, high current" [1], which accommodates interleaving techniques. In an interleaved converter, multiple phases are paralleled, and individual phases are active at spaced intervals equal to  $360^\circ/n$ , where  $n$  is the total number of phases [2]. Compared with a single-phase converter, it has advantages including higher efficiency, better dynamic response, better load regulation, and ease of maintenance [3]. Based on different objectives, the interleaved parallel system is controlled by different strategies. Among them, Current Sharing Control (CSC) and Thermal Balancing Control (TBC) are two widely used control methods.

The modular output currents of the multi-phase system are desired to be equal under CSC. If the output currents are well balanced, smaller filtering capacitors can be adopted in multi-phase systems. Hence, better dynamic response, and optimized system thermal distribution can be achieved [2]. CSC can be classified into droop methods and active current sharing methods [4]. Droop

This work was supported in part by the National Natural Science Foundation of China under Grant 52077140, and in part by the Shanghai Rising Star Program under Grant 20QA1406700.

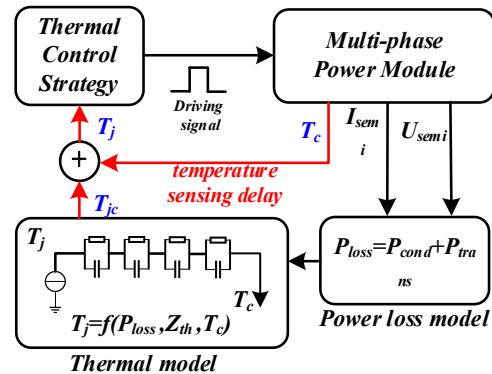


Fig. 1. Junction temperature estimation-based thermal management strategy.

methods change the load-regulation characteristic of paralleled power supplies and maintain a relatively balanced current distribution among phases [3]. However, droop methods cannot achieve favorable load regulation due to the lack of communication between the modules. On the other hand, active current sharing methods compensate for the output current mismatch between phases. Master-Slave CSC is one of the most popular active methods. It adjusts the output current of the slave converters to match the master's output current [5]. Nevertheless, once the master module fails, the entire system is unable to work normally. Another active method is average-current-sharing control. The output current of each phase is controlled to reach the average output current of paralleled modules [6]. However, evaluation of the control stability is complicated since the current equalization and voltage regulation are coupled.

Despite the above-mentioned benefits of CSC methods, the power loss of each module may vary unevenly. It can lead to a significant temperature mismatch under long-term operation with nonidentical switching device parameters. As a result, the uneven temperatures of the devices will degrade the overall system reliability [7]. To improve the reliability and to extend the lifetime of power electronic modules, it is necessary to balance the thermal stress of modules. Active thermal control (ATC) is an effective way to reduce the thermal stress of the components [8]. They utilize thermal variables to control the junction temperatures [9]. The temperature of power modules is essential, while it is difficult to measure [10-11]. However, the time delay between the heat source and

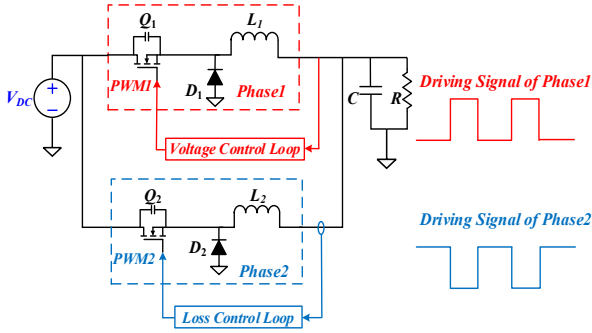


Fig. 2. Two-phase interleaved buck system.

sensed temperature is long. Therefore, temperature sensor-based thermal control is not favorable to fast dynamic control [12]. An alternative is junction temperature estimation, as is shown in Fig. 1, the power device case temperature and the thermal characteristic parameters are used to estimate the junction temperature [13]. However, the temperature is only a manifestation of heat, which is induced by power loss. Since temperature rise is proportional to heat, which is the integral of power loss, there is a delay between temperature and losses, which cannot be avoided by the method of junction temperature estimation. To improve, this paper proposes a heat equalization control method based on power loss model.

To make the interleaving parallel system possess a convenient thermal balancing control as well as a rapid dynamic response, this paper proposes a sensorless thermal balancing strategy. This work estimates the switching loss and proposes a closed-loop thermal balancing control for a two-phase interleaving Buck converter. To show the effect of the proposed method, the performance of CSC is also presented. Simulations and experiments are carried out to show the effectiveness and convenience of the proposed method.

## II. SYSTEM INTRODUCTION AND LOSS MODELING

### A. System Introduction

A two-phase interleaved Buck system is investigated as the case study. The schematic is shown in Fig. 2. The system consists of two-phase Buck modules, whose input and output ports are paralleled. Meanwhile, there is a  $180^\circ$  phase difference between the driving signals of the two Bucks.

Phase 1 is controlled by voltage-loop, while Phase 2 is controlled by loss-loop. Therefore, Phase 1 regulates the output voltage, while Phase 2 balances the power loss. Compared with single-phase buck converters, multi-phase converters are more suitable for high-power applications, because of the reduced capacitors and improved thermal performance. Additionally, since different phases are paralleled, it is easy to be extended to more phases, where one phase regulates the output voltage, and the other takes charge of the power loss balance.

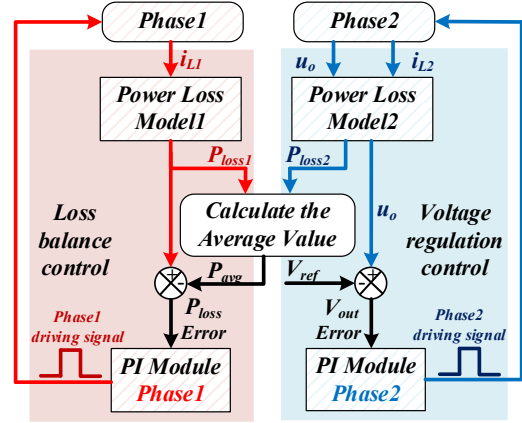


Fig. 3. Operation mechanism of the proposed loss balancing strategy.

### B. Loss Modeling

State-of-the-art thermal balance control methods either require temperature sensing with severe delay to feedback temperature or require complicated junction temperature estimation [14]. This work controls the loss of each module to achieve a simple thermal balance with a fast-dynamic response. In other words, loss balance control is used to complete the thermal equalization control.

Loss model is an important part of loss equalization control. The loss in Buck module is mainly caused by power semiconductor devices, for example, power MOSFETs and power diodes. For these devices, conduction loss and switching loss are the main components of the loss. Based on the above analysis, the loss model is listed in (1-3).

$$P_Q(t) = i_Q(t)^2 R_{ds(on)} + 0.5V_{in} I_o f_s (t_r + t_f) \quad (1)$$

$$P_D(t) = i_D(t)^2 R_D + i_D(t)V_D \quad (2)$$

$$P_{Semi}(t) = P_Q(t) + P_D(t) \\ = i_Q(t)^2 R_{ds(on)} + 0.5V_{in} I_o f_s (t_r + t_f)^2 \\ + i_D(t)^2 R_D + i_D(t)V_D \quad (3)$$

where,  $P_Q$  is the loss of power MOSFET,  $P_D$  is the power of the power diode, and  $P_{Semi}$  represents the total loss of power semiconductors. The loss model includes the switching loss and conduction loss of power MOSFET and the conduction loss of power diode.

Parameter descriptions are as follows:  $i_Q$  -- MOSFET current;  $R_{ds(on)}$  -- MOSFET on resistance, which can be got from the data sheets;  $V_{in}$  -- input voltage;  $I_o$  -- output current;  $f_s$  -- switching frequency;  $t_r$  -- MOSFET rising time,  $t_f$  -- MOSFET falling time, both  $t_r$  and  $t_f$  can be read from the data sheets;  $i_D$  -- diode current;  $R_D$  -- diode equivalent resistance;  $V_D$  -- diode forward voltage, which can also be extracted from the datasheets.

## III. PROPOSED THERMAL MANAGEMENT STRATEGY

To achieve an even thermal distribution of the interleaving system without temperature sensors, a loss-

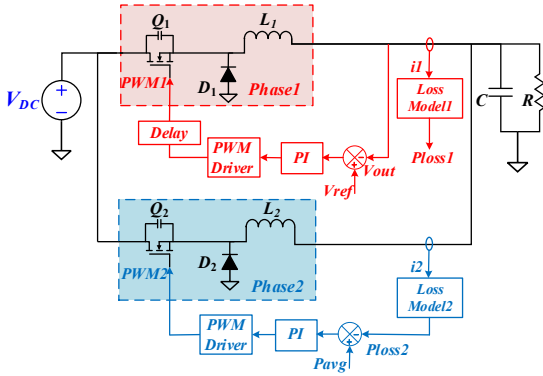


Fig. 4. Temperature sensorless thermal balance control scheme.

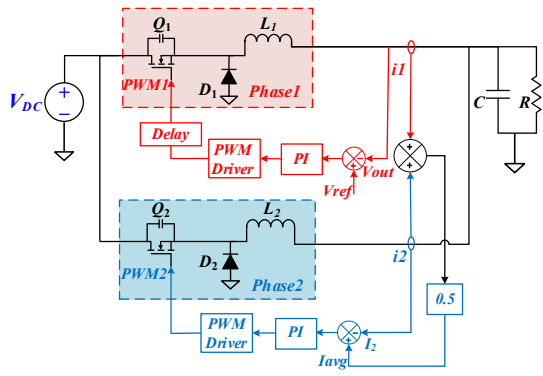


Fig. 5. Improved current sharing control scheme.

balance methodology is proposed. It does not require temperature sensors or junction temperature estimation of power semiconductors. To compare the thermal balance performance of the proposed temperature sensing free-thermal balance methodology, simulations and experiments of CSC are carried out. This paper also proposes an improved CSC method that decoupled the voltage control loop and current control loop. This section describes the two balance control strategies. The operation mechanism of the proposed loss balancing strategy is shown in Fig. 3.

#### A. Proposed Loss Balancing Strategy

The diagram of the loss balancing strategy is shown in Fig. 4. Aiming at achieving balanced loss and regulated output voltage simultaneously, one Buck converter controls the loss, and the other stabilizes the output voltage.

Phase 1 regulates the system's output voltage, so the input of the PI compensation in this phase is the error between the actual output voltage and the reference voltage, and the PI loop stabilizes the output voltage to the desired value. Phase 2 aims to balance the switching loss of the two modules. Therefore, the input of the PI compensation of this phase is the error between the calculated loss and the average loss. By sampling the output current of the two Bucks, and then inserting the current values into (3), the switching loss of each Buck can be obtained separately. The reference of the loss is the average loss.

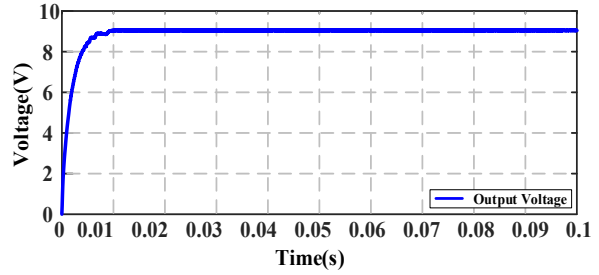


Fig. 6. Simulation results of the output voltage by the proposed thermal balance control.

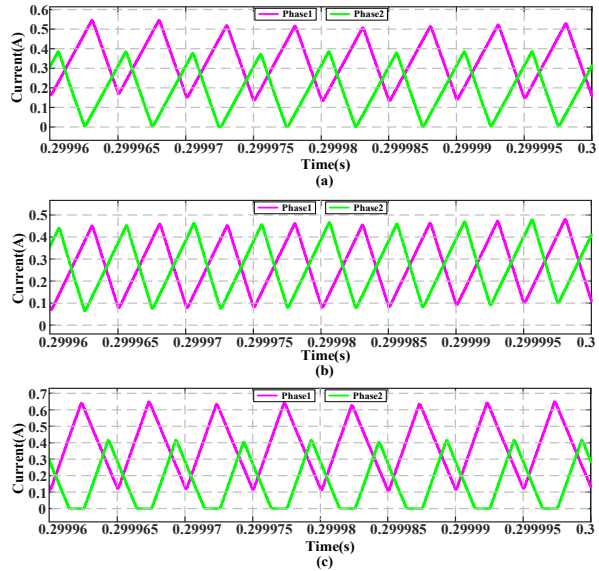


Fig. 7. Simulation results of inductor current under (a)VRC, (b)CSC and (c)the proposed thermal balance control.

TABLE I  
Simulation Parameters

	MOSFET $R_{(on)}$	Diode $R_{(on)}$	L	$C_{out}$	input voltage	output voltage
Phase1	2.5m $\Omega$	0.6 $\Omega$	47 $\mu$ H	47 $\mu$ F	15V	9V
Phase2	10 $\Omega$	0.8 $\Omega$				

#### B. Improved Current Sharing Control Strategy

The conventional average-current-sharing control method adds the voltage error and current error, and makes the sum of the errors the input of PI compensation. Therefore, when the polarity of current error and voltage error is opposite, the control signal often cannot make the system achieve current balance and stabilized output voltage at the same time, and the system tends to lose its stability. In this paper, the average-current-sharing control method is improved by decoupling current control and voltage control. In other words, one phase is responsible for current balancing and the other phase aims at stabilizing the output voltage. The diagram is shown in Fig. 5.

### IV. SIMULATION AND ANALYSIS

Simulation is carried out in SIMULINK, and this section shows the simulation results of voltage regulation control(VRC), CSC, and the proposed temperature sensorless thermal balance control. To show the effect of

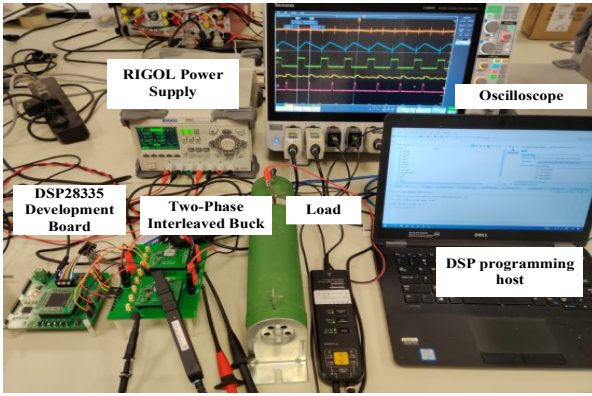


Fig. 8. Picture of the experimental platform.

TABLE II  
Experiment Parameter Design

	L	$C_{out}$	MOSFET	Power Diode
Phase1	47 $\mu$ H	47 $\mu$ F	BSC031N06NS3G $R_{ds(on)}=3.1m\Omega$	SVM1550UB
Phase2	47 $\mu$ H	47 $\mu$ F	BSC123N08NS3G $R_{ds(on)}=12.3m\Omega$	SVM1550LB

CSC, the simulation of VRC is also carried out. The simulation conditions are shown in Table I.

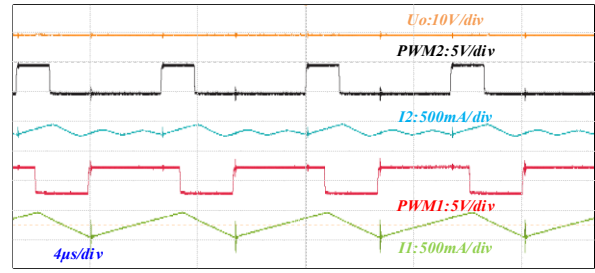
The output voltage of the system can be stabilized at the design value of 9V by VRC, CSC, and the proposed thermal balance control, which indicates that the three closed loops can stabilize the output voltage. Fig. 6 shows the output voltage by the proposed thermal balance control. Fig. 7(a)~Fig. 7(c) show the inductor current under VRC, CSC, and the proposed thermal balance control respectively. The average inductance current of Phase 1 in Fig. 7(a) is 0.339A, and that of Phase 2 is 0.190A, while the average inductance current of Phase 1 in Fig. 7(b) is almost equal to that of Phase 2 at the steady-state, which is 0.265A. It can be concluded that the proposed CSC can make the output current of the two phases tend to be equal. The loss of the switching devices in the two Bucks can also be obtained, under CSC, the loss of phase 1's switching devices is 19.76mW, and that of Phase 2 is 64.10mW. However, under the proposed thermal balance control, the loss of Phase 1's switching devices is 51.95mW, and that of Phase 2 is 48.03mW. It is proved that the proposed thermal balance control can equalize the loss of the switching devices in the two-phase interleaved Buck system.

## V. EXPERIMENTAL RESULTS

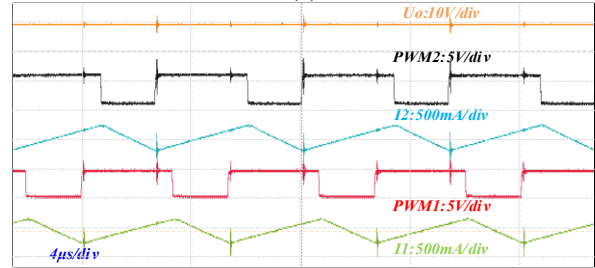
A two-phase interleaved Buck system is designed, and TMS320F28335 is used to implement the control algorithm in experiments. Fig. 8 shows the experimental platform.

### A. Experiment conditions and device selection

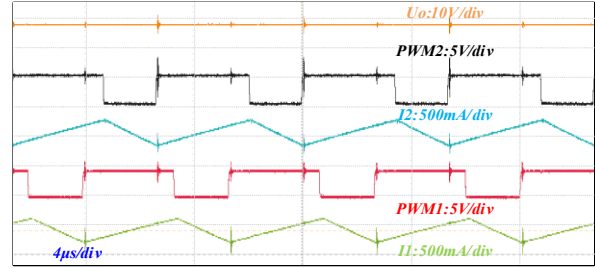
The input voltage of the system is 15V, the output voltage is 9V, the load is 8.5 $\Omega$ , and the switching frequency is 200kHz. The parameter design is listed in Table II.



(a)



(b)



(c)

Fig. 9. The output voltage, switch driving waveform and inductance current of each phase under different control strategies. (a)Results for VRC. (b) Results for CSC. (c)Results for the proposed thermal balance control.

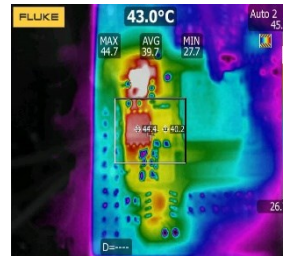


Fig. 10. Phase 1's average temperature of the switching devices under the proposed thermal balance control.

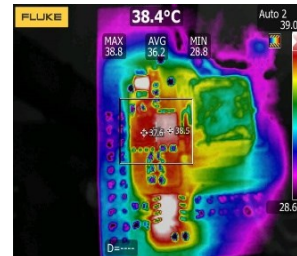


Fig. 11. Phase 2's average temperature of the switching devices under the proposed thermal balance control.

### B. Experiment results

Output voltage, driving waveform, and inductance current waveform of each phase under different control strategies can be observed by oscilloscope. Meanwhile, the thermal equalization effect of the proposed thermal balance control can be observed by the thermal imager. The experiment results are shown in Table II, Fig. 9, Fig. 10, and Fig. 11.

It can be seen from Fig. 9(a-c) that under the three control strategies, the output voltage can be stabilized at 9V, which indicates that the proposed current sharing control method and the proposed thermal balance method

TABLE III  
The average temperature of the switching devices

Control Strategy	Phase	Average Temperature of Switching Devices (°C)
VRC	1	43.7
	2	30.5
CSC	1	41.5
	2	34.4
The Proposed Thermal Balance Control	1	39.7
	2	36.2

can stabilize the output voltage of the two-phase interleaved Buck system.

By comparing Fig. 9(a) and Fig. 9(b), the average of the inductance current of Phase 1 in Fig. 9(a) is 1.108A, the average inductance current of Phase 2 is 27.79mA, and the average inductance current of Phase 1 in Fig. 9(b) is 536.0mA, and that of Phase 2 is 580.6mA. This shows that the proposed current sharing method can balance the output current of each module effectively.

Table III shows the average temperature of the switching devices for the two-phase interleaved Buck system under three control strategies. It can be seen that the temperature difference of the two phases at CSC is smaller than that of VRC, while the difference is minimized at the proposed thermal balance control.

Fig. 10 and Fig. 11 show the average temperature of the switching devices of the two-phase Buck under the proposed thermal balance control. It can be seen from Table III, Fig. 10, and Fig. 11 that compared with VRC, CSC can relieve the thermal management pressure of the multi-module system to some extent. That is, the temperature difference between modules in this case is smaller than that under VRC. However, in the proposed thermal balance control mode, the average temperature of the two phases' switch tubes is minimized, which are 39.7°C and 36.2°C, respectively. The temperature difference between the two phases is 13.2°C under VRC, 7.1°C under CSC, and 3.5°C under the proposed thermal balance control. This verifies thermal equalization through proposed temperature sensorless thermal balance control and shows that the module heating can be effectively controlled by adjusting the loss of the main power devices.

## VI. CONCLUSION

To avoid the lagged process of temperature sensing and the complex junction temperature estimation, this paper proposes a method to realize the thermal balance control by equalizing the losses of the main power devices in a multi-phase buck system.

Firstly, the loss of switching devices is estimated for a two-phase interleaved buck system. Secondly, based on the traditional average current method, a CSC method with decoupled voltage loop and current loop and the proposed thermal balance control are proposed. Then, the simulation and experiment of VRC, CSC, and the proposed thermal balance control are carried out. The results prove that the proposed CSC can effectively balance the output current of two modules, and the

proposed thermal balance control can make the average temperature of switching devices of each phase closer.

It can be concluded that without using temperature sensors with large delay and complex junction temperature estimation, the proposed thermal balance control proposed can effectively balance the temperature of each module. While this paper does not take the tolerance of the device parameters into consideration, such as  $R_{ds}$ ,  $R_D$ ,  $V_D$ , and so on, which may influence the accuracy of the power loss model. To solve this issue, a Monte Carlo simulation can be used, where device parameters are considered as normal distribution to emulate a real operation environment [15].

## REFERENCES

- [1] J. Gordillo and C. Aguilar, "A simple sensorless current sharing technique for multiphase DC-DC buck converters," *IEEE Trans. Power Electron.*, vol. 32, no. 5, pp. 3480–3489, May.2017.
- [2] C. Parisi, "Multiphase buck design from start to finish (Part 1)," 2021. [Online]. Available: [www.ti.com](http://www.ti.com).
- [3] V. P. Oberio, M. D. Depexe, T. C. Naidon, and A. Campos, "An improved droop control strategy for load current sharing in output parallel-connected DC-DC converters," in *Proc. 11th IEEE/IAS Int. Conf. Ind. Appl.(INDUSCON)*, Juiz de Fora, Brazil, Dec.2014, pp. 1–7.
- [4] S. Luo, Z. Ye, R. L. Lin, and F. C. Lee, "A classification and evaluation of paralleling methods for power supply modules," in *Proc. IEEE Power Elect. Spec. Conf.*, Charleston, SC, USA, Jul.1999, pp. 901–908.
- [5] H. C. Chen, C. Y. Lu, and U. S. Rout, "Decoupled master-slave current balancing control for three-phase interleaved boost converters," *IEEE Trans. Power Electron.*, vol. 33, no. 5, pp. 3683–3687, May.2018.
- [6] C. Pengming, D. Guo, S. Chao, C. Handong, and X. Guoying, "Stability analysis of identical paralleled DC-DC converters with average current sharing," in *Proc. 2019 IEEE Asia Power and Energy Engineering Conference (APEEC)*, Chengdu, China, May.2019, pp. 60–64.
- [7] S. Kalker et al., "Reviewing thermal monitoring techniques for smart power modules," *IEEE J. Emerg. Sel. Top. Power Electron.*, vol. 6777, Mar.2021.
- [8] M. Andresen, K. Ma, G. Buticchi, J. Falck, F. Blaabjerg, and M. Liserre, "Junction temperature control for more reliable power electronics," *IEEE Trans. Power Electron.*, vol. 33, no. 1, pp. 765–776, Jan.2018.
- [9] J. Falck, M. Andresen, and M. Liserre, "Active thermal control of IGBT power electronic converters," in *Proc. IECON 2015 - 41st Annu. Conf. IEEE Ind. Electron. Soc.*, Yokohama, Japan, Jan.2016, pp. 1–6.
- [10] M. Andresen, M. Schloh, G. Buticchi, and M. Liserre, "Computational light junction temperature estimator for active thermal control," in *Proc. IEEE Energy Convers. Congr. Expo. (ECCE)*, Milwaukee, WI, Sept.2016, pp. 1–7.
- [11] Falck, G. Buticchi, and M. Liserre, "Thermal stress based model predictive control of electric drives," *IEEE Trans. Ind. Appl.*, vol. 54, no. 2, pp. 1513–1522, Apr.2018.
- [12] P. K. Prasobhu, V. Raveendran, G. Buticchi, and M. Liserre, "Active thermal control of GaN-Based DC/DC Converter," *IEEE Trans. Ind. Appl.*, vol. 54, no. 4, pp. 3529–3540, Aug.2018.
- [13] R. Han et al., "Thermal stress balancing oriented model predictive control of modular multilevel switching power amplifier," *IEEE Trans. Ind. Electron.*, vol. 67, no. 11, pp. 9028–9038, Nov.2020.
- [14] X. Han and M. Saeedifard, "Junction temperature estimation of SiC MOSFETs based on Extended Kalman Filtering," in *Proc. IEEE Appl. Power Electron. Conf. Expo. (APEC)*, San Antonio, TX, USA, Mar.2018, pp. 1687–1694.
- [15] M. Liserre, V. Raveendran and M. Andresen, "Graph-Theory-Based Modeling and Control for System-Level Optimization of Smart Transformers," *IEEE Trans. Ind. Electron.*, vol. 67, no. 10, pp. 8910–8920, Oct. 2020.